



Power Electronic Systems  
Laboratory

© 2023 IEEE

Proceedings of the IEEE International Conference on Compatibility, Power Electronics and Power Engineering (CPE-POWERENG 2023), Tallinn, Estonia, June 14-16, 2023

## **Single-/Three-Phase Bidirectional EV On-Board Charger Featuring Full Power/Voltage Range and Cost-Effective Implementation**

H. Sarnago,  
O. Lucia,  
D. Menzi,  
J. W. Kolar

Personal use of this material is permitted. Permission from IEEE must be obtained for all other uses, in any current or future media, including reprinting/republishing this material for advertising or promotional purposes, creating new collective works, for resale or redistribution to servers or lists, or reuse of any copyrighted component of this work in other works



Eidgenössische Technische Hochschule Zürich  
Swiss Federal Institute of Technology Zurich

# Single-/Three-Phase Bidirectional EV On-Board Charger Featuring Full Power/Voltage Range and Cost-Effective Implementation

Héctor Sarnago<sup>1</sup>, *Senior Member, IEEE*, Óscar Lucía<sup>1</sup>, *Senior Member, IEEE*,  
David Menzi<sup>2</sup>, *Member, IEEE*, Johann W. Kolar<sup>2</sup>, *Fellow, IEEE*.

<sup>1</sup>Department of Electronic Engineering and Communications.  
I3A. Universidad de Zaragoza  
Zaragoza, Spain.  
olucia@unizar.es

<sup>2</sup>Power Electronic Systems Laboratory  
ETH Zurich  
Zurich, Switzerland  
menzi@lem.ee.ethz.ch

**Abstract**— On-board chargers (OBC) are required to operate under a wide range of operating conditions in terms of input voltage, phase number, and output battery voltage. Accordingly, achieving a high-performance, efficient and cost-effective implementation poses special challenges. In this paper, a novel OBC architecture is considered which is able to operate both in three-phase and single-phase configuration with full output power range without requiring additional power components or degrading performance. The proposed solution provides a universal-charging single-power-processing block that features a high power density and cost-effective implementation. In this paper, a bidirectional 11-kW 800-V battery voltage prototype of the system is designed and constructed for a 400V (line-to-line) mains supply.

**Keywords**—Electric vehicle, on-board charger, power electronics.

## I. INTRODUCTION

Electric vehicles (EVs) are a key element in a transition towards electrification in a vast number of sectors that will contribute to a more environmentally friendly sustainable development. Among the new technologies present in such vehicles, battery-related power electronics plays a key role in ensuring a high-performance, efficient, and safe operation. In particular, on-board chargers (OBCs) [1] provide the required dc current to charge the battery in a wide range of input and output conditions, which depends on the single-/multi-phase mains voltage, the battery technology and the battery state of charge.

The first modern technology successfully developed for battery electric vehicles (BEV), and still the most widely adopted, is based on 400V high voltage batteries. This technology employed OBCs that can typically operate in a 250V to 450V range using 600V power semiconductors. Unidirectional operation, i.e., only battery charging, was considered so far, and these devices are often implemented using a modular approach for each phase comprising three single-phase unity power factor ac-dc front-end converters (Fig. 1 (a)) [2]. This approach, however, requires dedicated isolating transformers and dc-dc power converters. Besides, the control architecture, the sensing circuits and the power supply design are complex due to the required multiple isolation barriers and power reference considerations. All these elements combined lead to performance degradation, reduced power density, and increased cost. In recent years, technology and market requirements towards higher power

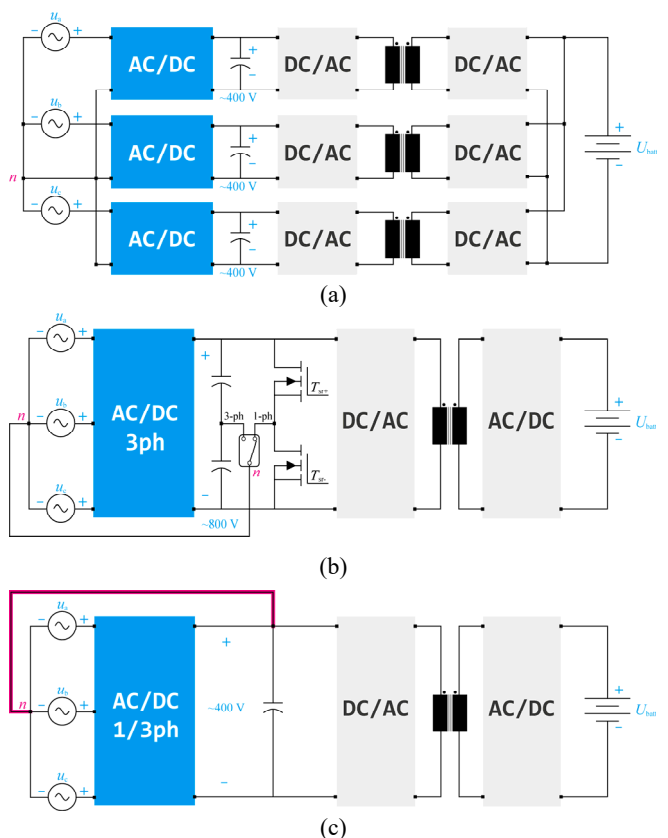


Fig. 1. On-board charger architectures comprising a unity power factor ac-dc front-end and a subsequent isolated dc-dc converter: (a) phase modular and (b) single front-end stage architectures converting three-phase ac voltages  $u_a$ ,  $u_b$ ,  $u_c$  (or alternatively a single-phase voltage  $u_{abc}$ ) to an isolated dc output voltage  $U_{\text{batt}}$ ; and (c) proposed single-/three-phase single-front-end stage achieving 400V output voltage.

ratings, combined with advances in battery and SiC power semiconductor technology, both in terms of performance and cost, have led to the adoption of 800V batteries [3, 4]. This enables to reduce the current in the EV motor and the fast charging system, leading to more efficient and higher power density implementations. The adoption of 1200V SiC devices has made possible also the use of single front-end three-phase rectifiers that enable a low complexity and low component-count implementation (Fig. 1 (b)). This evolution has been made in combination with the need for bidirectional power conversion to enable OBCs that can cope with modern

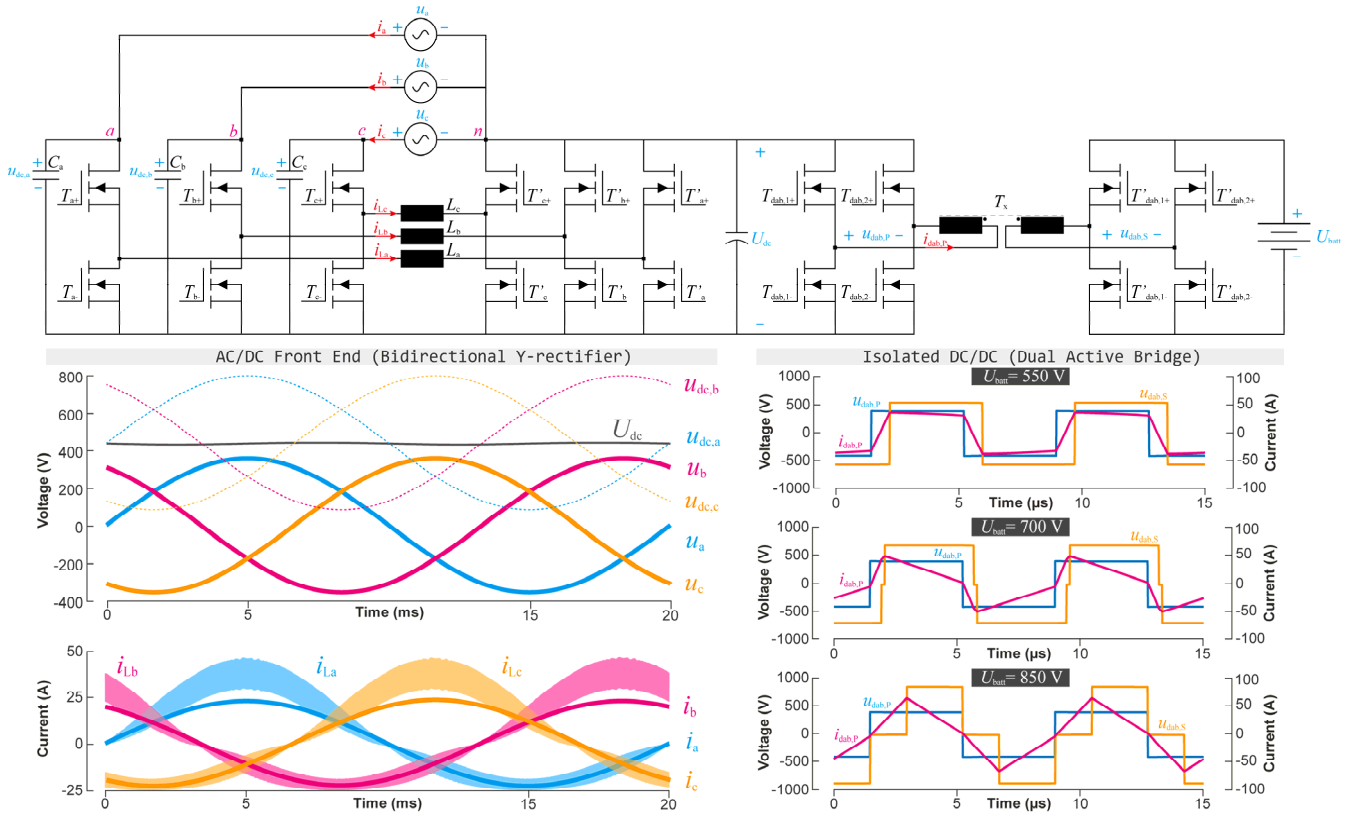


Fig. 2. Proposed bidirectional OBC architecture in three-phase operation (top), and main ac-dc front-end waveforms within one grid period (bottom left) and main dc-dc waveforms under different battery voltage conditions within one switching period (bottom right).

vehicle-to-home (V2H), vehicle-to-vehicle (V2V) and/or vehicle-to-load (V2L) charging standards [4].

Despite these advances, currently implemented architectures still suffers from several limitations when operating in a wide range of input and output conditions. In particular, operation in single-phase configuration (or split-phase operation) is challenging for three-phase rectifiers [5], requiring an additional current path (Fig. 1 (b)), using high voltage diodes or MOSFETs in the case of bidirectional operation. This results in lower power conversion efficiency and requires the use of additional power electronic components when compared to three-phase operation. Additionally, the high intermediate dc-link voltage of these boost-type three-phase rectifiers, typically 750...850V [6], disadvantageously prevents the use of high power-density electrolytic capacitor technology, usually rated only up to 450V. As a result, a series connection is usually adopted, requiring additional circuitry for voltage supervision and/or balancing.

In this context, this paper aims at providing a universal single-/three-phase solution for bidirectional EV charging. To achieve this, a new OBC architecture (Fig. 1 (c)) is investigated which is based on the boost-type rectifier from [7] that, unlike previous proposals, enables *both* three-phase *and* single-phase operation with full operating range with no required additional power devices or penalties in the device stress [8]. Additionally, the 400V intermediate dc-link voltage simplifies the use of electrolytic capacitor technology to decouple the grid power pulsation in single-phase operation. Then, a full-bridge-based dual active bridge (DAB) converter [9] completes the OBC to provide isolation, to adapt the intermediate dc-link voltage to the battery voltage  $U_{\text{batt}}$ , and to enable a fully bidirectional operation.

The remainder of this paper is organized as follows: Section II details the considered OBC architecture, describing the rectifier operation in three-phase *and* single-phase configuration and the operation of the isolated dc-dc converter. Section III shows a 3D-CAD rendering of the constructed prototype, and presents the main experimental waveforms and efficiency measurement results. Finally, section IV summarizes the main contributions of the paper.

## II. ON-BOARD CHARGER ARCHITECTURE

The considered OBC power converter architecture is based on the single-/three-phase ac-dc front-end from [8] combined with an isolated DAB dc-dc converter.

### A. AC-DC Front-End

The proposed differential rectifier is based on the phase-modular buck-boost Y-rectifier [7] and comprises three identical input stages, each one comprising a buck-boost dc-dc converter structure connected to a common star "Y" point given by the negative dc-link rail. As proposed in [8] the grid neutral point  $n$  is connected to the positive intermediate dc-link rail  $U_{\text{dc}}$ . Each phase is composed of an ac-side half-bridge leg, connected to the corresponding grid terminal (which shows a positive voltage against the Y-rail), and a dc-side half-bridge leg, connected to the positive dc output rail (and hence also to the grid neutral point), allowing both three- and single-phase operation. In the case of three-phase operation (Fig. 2), grid phase voltages,  $u_a$ ,  $u_b$ , and  $u_c$ , are connected to the ac-side terminals  $a$ ,  $b$ , and  $c$ , respectively and the converter realizes sinusoidal grid currents  $i_a$ ,  $i_b$ , and  $i_c$  in phase with the respective grid voltages.

The basic operating concept is identical for all phases, and is hence only explained for phase  $a$ , depicted in Fig. 4. The

module structure is formed by the ac- and dc-side half-bridge transistors  $T_{a+}, T_{a-}, T'_{a+}, T'_{a-}$ . Two different exclusive operating modes can be distinguished within one grid period:

a) *Mode I*: When the grid voltage is positive,  $u_a > 0$ , the converter operates in a first mode, being the ac-side half-bridge transistors  $T_{a+}, T_{a-}$ , complementary switched and  $T'_{a+}$  continuously activated. Assuming the switching frequency is much higher than the grid frequency,  $f_{sw} \gg f_{ac}$ , the ac-stage ac-side half-bridge duty cycle,  $d_a$ , results as

$$d_a(t) = \begin{cases} \frac{U_{dc}}{U_{dc} + u_{dc,a}(t)}, & u_a(t) \geq 0 \\ 1, & u_a(t) < 0 \end{cases}, \quad (1)$$

where the input capacitor voltage of the ac-side half-bridge is the sum of the intermediate dc-link voltage and the grid phase voltage,  $u_{dc,a} = U_{dc} + u_a$ . In order to ensure proper converter operation a strictly positive input capacitor voltage is required,  $u_{dc,a} > 0$ , resulting in  $U_{dc} = 400 \dots 450V$ , for universal grid operation with a wide grid line-to-neutral voltage range of  $U_{ac} = 85 \dots 265V_{RMS}$ . As a consequence, 600V rated power devices can be used for the dc-side half-bridge legs, whereas 1200V SiC MOSFETs are required for the ac-side half-bridge legs ( $U_{dc,a,max} = U_{dc} + U_{a,pk} = 520 \dots 825V$ ), independently of the operation in single-phase or three-phase mode.

b) *Mode II*: Opositely, when the grid voltage is negative,  $u_a < 0$ , the converter operates in a second mode, by switching the dc-side half-bridge MOSFETs  $T'_{a+}, T'_{a-}$ , with the upper transistor of the ac-side half-bridge  $T_{a+}$  continuously

activated. In this case, the resulting ac-side half-bridge duty cycle,  $d'_a$ , is

$$d'_a(t) = \begin{cases} 1, & u_a(t) \geq 0 \\ \frac{U_{dc} + u_{dc,a}(t)}{U_{dc}}, & u_a(t) < 0 \end{cases}. \quad (2)$$

The applied duty cycle profiles, shown Fig. 4 result in a mutually exclusive high-frequency switching operation of ac- and dc-stage, such that only three out of six half-bridges are switched simultaneously in the entire ac-dc front-end, thus reducing switching losses.

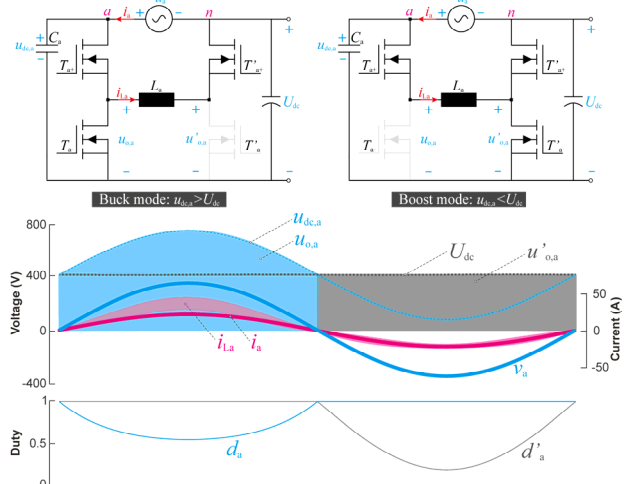


Fig. 4. Operating modes of the ac-dc front-end module a (top), and corresponding converter waveforms (middle), and modulation parameters (bottom).

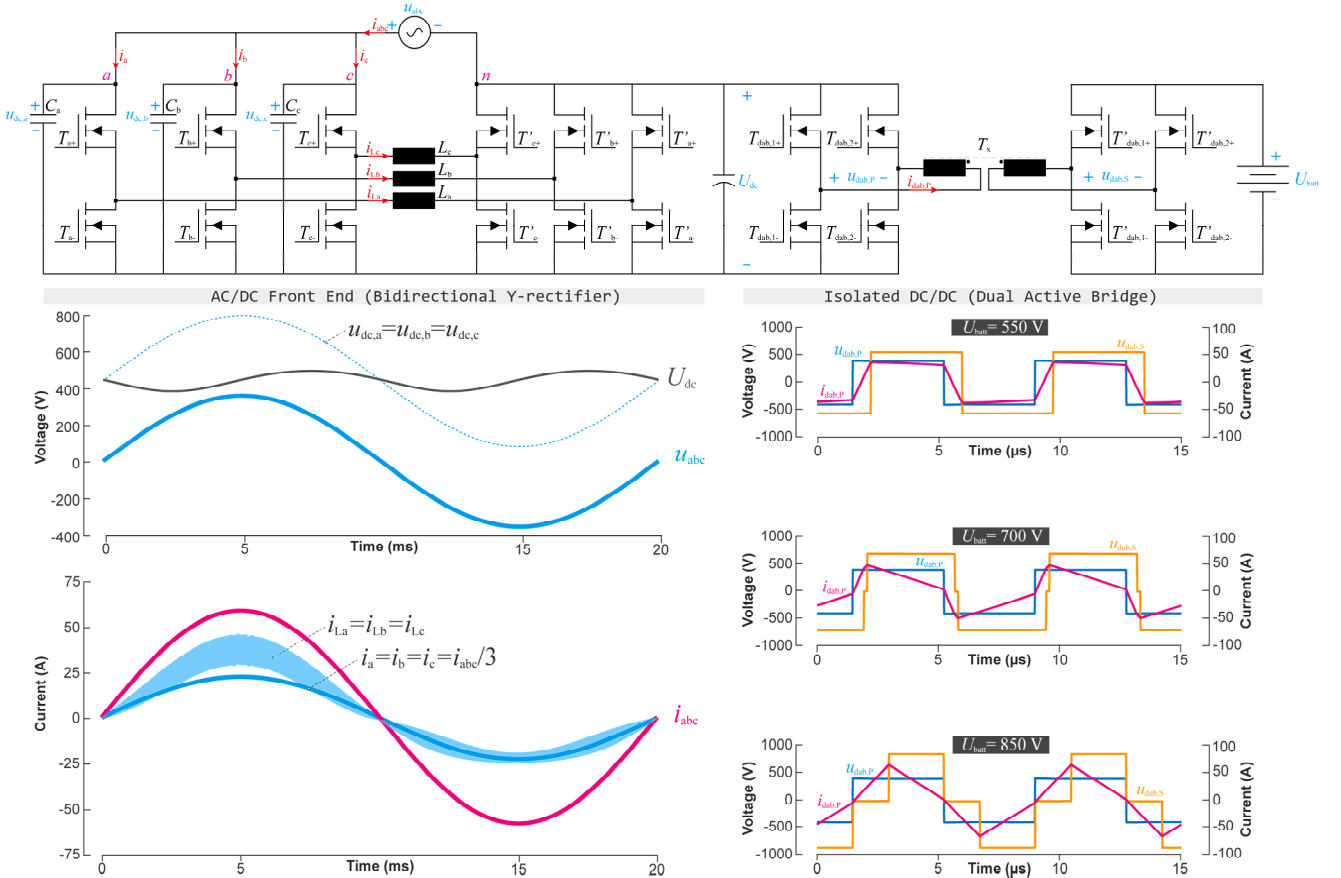


Fig. 3. Proposed bidirectional OBC architecture in single-phase operation (top), and corresponding main ac-dc front-end waveforms within one grid period (bottom left) and main dc-dc waveforms under different battery voltage conditions within one switching period (bottom right).

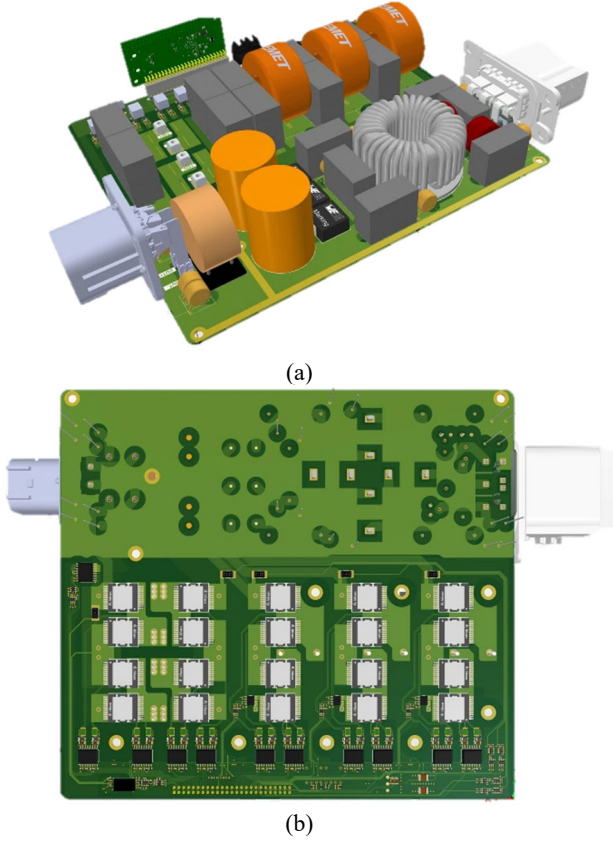


Fig. 5. 3D rendering of the OBC prototype: top (a) and bottom (b) views.

The proposed converter, in contrast to the phase-modular buck-boost Y-rectifier [7], advantageously connects the grid neutral point  $n$  with the intermediate dc-link bus,  $U_{dc}$ . In case of single-phase operation (Fig. 3), the grid voltage  $u_{abc}$  is connected to the parallel-connected ac-side terminals  $a$ ,  $b$ , and  $c$  such that the current is equally shared among the phase modules, being  $i_a = i_b = i_c = i_{abc}/3$ . The aforementioned connection of the grid neutral point and the positive intermediate dc-link creates a return path for the single-phase grid current  $i_{abc}$ . This represents one of the main advantages of the proposed converter over previous proposals, since it allows full output power range operation in both three-phase *and* single-phase operation without over-dimensioning power devices or requiring additional elements. Besides, both ac- and dc-side half-bridge legs are referenced to the same point, simplifying the isolation considerations and control architecture.

### B. Dual Active Bridge DC-DC Converter

Finally, the OBC architecture is completed with a single DAB dc-dc converter that provides isolation. In contrast to the buck-boost Y-rectifier [7], the ac-dc front-end from [8] is limited to boost operation and hence the DAB converter has to adapt the intermediate dc-link voltage  $U_{dc}$  to the voltage in the high-voltage battery  $U_{batt}$ . This converter is composed of a primary-side full-bridge,  $T_{dab,1,2}$  and a secondary-side full-bridge,  $T'_{dab,1,2}$  whose modulation allows bidirectional power transfer and adapting the operating conditions to the battery voltage. Compared to the state-of-the-art modular approach (Fig. 1(a)), the proposed converter achieves the required isolated power conversion using a single dc-dc converter,

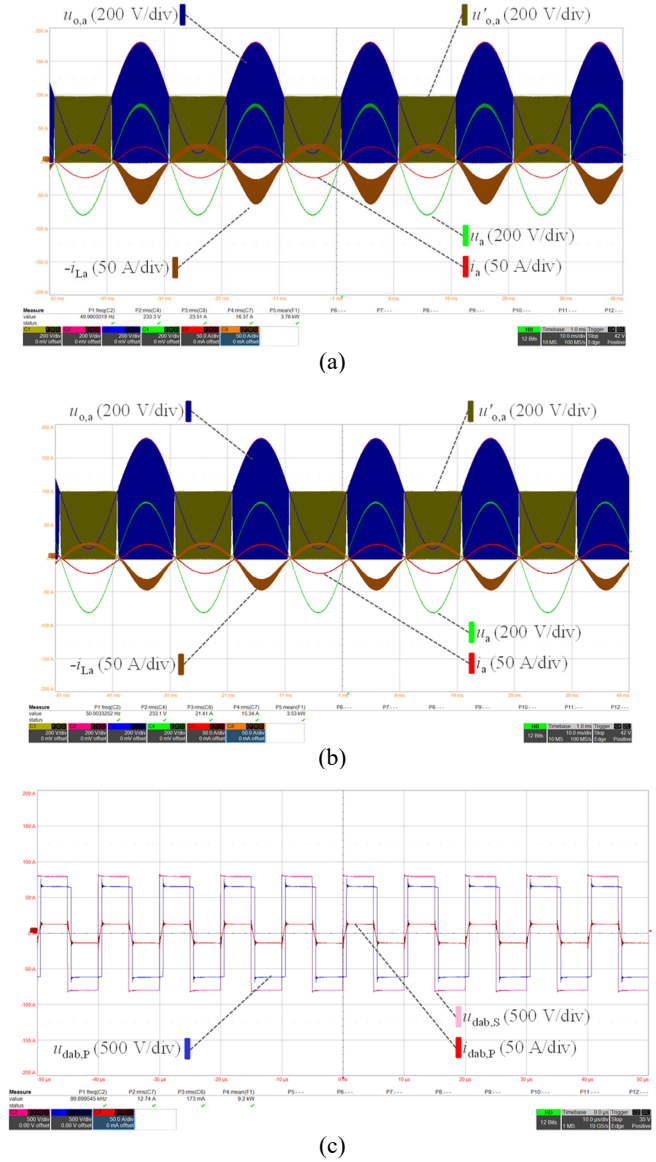


Fig. 6. Main experimental results of the considered OBC architecture: ac-dc front-end for  $U_{ac}=230$  V<sub>RMS</sub> operating with 16 A input phase current at 50 kHz (a) and 100 kHz (b). In each figure, from top to bottom: ac- and dc-side half-bridge switch-node voltage (200 V/div), grid voltage (200 V/div), grid current (50 A/div) and inductor current (50 A/div). High-frequency DAB converter waveforms for  $U_{batt}=800$  V and a transferred power of 9.2 kW (c). Full-bridge switch-node voltages (500 V/div) and transformer primary-side current (50 A/div).

reducing the number of power devices, magnetic components and further simplifying the isolation and control architecture.

In order to adapt the 400V intermediate dc-link voltage to the wide-range 800V battery voltage,  $U_{batt}=550\dots850$ V,  $n=1.34$  has been selected as optimum transformer turns ratio. Consequently, pseudo-trapezoidal operation can be used for the lower battery voltage range, resulting in a minimum conduction loss for the most current-demanding operating condition (battery fully discharged). Additionally, full ZVS soft-switching behavior is obtained in both the primary- and secondary-side full-bridge. To minimize losses in the medium-to-high battery voltage operating range, secondary duty cycle variation has been also applied, as described in [10] as optimal modulation profile. All these modulations profiles have been depicted both in Fig. 2 and Fig. 3.

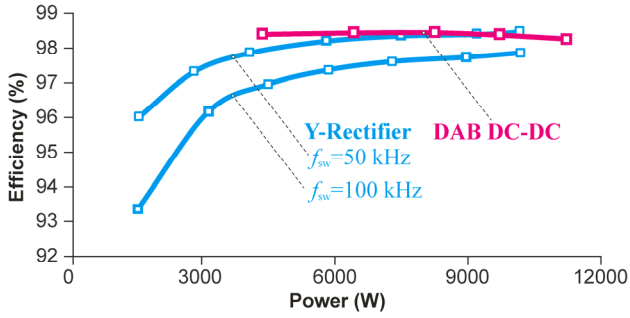


Fig. 7. Measured efficiency over input power for  $U_{ac}=230V_{RMS}$  (mains phase voltage),  $U_{dc}=800V$  and  $U_{batt}=800V$ : ac-dc front-end efficiency (for a switching frequency of 50kHz and 100kHz) and DAB dc-dc converter (for a switching frequency of 100kHz).

### III. IMPLEMENTATION AND EXPERIMENTAL RESULTS

In order to prove the feasibility of the proposed OBC architecture, an 11kW bidirectional prototype has been designed and implemented featuring an input voltage range of  $U_{ac}=85\dots265V_{RMS}$  (phase voltage) in both three-/single-phase operation. The DAB dc-dc stage has been designed to supply 800V high-voltage batteries with a voltage varying from 550V up to 850V.

The designed prototype uses 1200V & 750V SiC trench MOSFETs devices from Infineon in the rectifier stage. The DAB converter is implemented using 16m $\Omega$  750V SiC MOSFET in the primary-side and 20m $\Omega$  1200V SiC MOSFETs in the secondary-side stage. All these devices are top side cooled featuring QDPAK package for better thermal performance. The power semiconductors are digitally controlled using an FPGA (Artix 7-100T from Xilinx). Fig. 5 shows a 3D rendering of the designed prototype (not including the DAB converter transformer which is connected externally); whose dimensions are 239x216x58mm<sup>3</sup> (3.0dm<sup>3</sup>, 3.7kW/dm<sup>3</sup>, 60W/in<sup>3</sup>).

The ac-dc front-end converter has been tested at a switching frequency of 50kHz and 100kHz to verify its correct operation and perform an efficiency analysis. Fig. 6 shows the main experimental results of the proposed converter, illustrating the correct operation of the ac-dc front-end operating at 16 A input phase current at 50kHz (a) and 100kHz (b). In these figures, the grid voltage and current, the inductor current, and the ac- and the dc-stage high-frequency switch-node voltage of phase *a* can be seen. Additionally, the high frequency waveforms of the DAB converter at 9.2kW are also shown in Fig. 6 (c).

Finally, Fig. 7 shows efficiency measurement results obtained in the full output power range, i.e., up to 3.6kW per phase (a total input power of 11kW). The considered ac-dc front-end achieves peak efficiency values above 98% and 97% for operation with 50kHz and 100kHz switching frequency, respectively, whereas the DAB converter efficiency is close to 98.5%.

### IV. CONCLUSIONS

On-board chargers (OBCs) are an essential part of the electric vehicle (EV) power conversion architecture and are required to operate under a wide range of operating

conditions. New requirements in terms of single- and three-phase nominal power operation and bidirectionality, as well as the transition towards higher voltage batteries, bring new challenges to this field. This paper presents a new OBC architecture composed of a boost-type single-/three-phase front-end converter based on the buck-boost Y-rectifier and a dual active bridge (DAB) dc-dc converter. The considered OBC architecture, unlike previous proposals, provides full output power range both in three-phase and single-phase operation without requiring additional elements or power component over-dimensioning. Besides, the considered architecture provides additional benefits in terms of cost, control, and electromechanical integration due to the single-stage implementation and simplification in terms of isolation and control architectures. The concept has been tested using an 11kW bidirectional three-/single-phase OBC, thereby proving the feasibility of the system approach.

### ACKNOWLEDGEMENT

This work was partly supported by Projects PID2019-103939RB-I00 and TED2021-129274B-I00 co-funded by MCIN/AEI/10.13039/501100011033 and by the EU through FEDER and NextGenerationEU/PRTR programs, and by the DGA-FSE.

### REFERENCES

- [1] M. Yilmaz, and P. T. Krein, "Review of battery charger topologies, charging power levels, and infrastructure for plug-in electric and hybrid vehicles," *IEEE Transactions on Power Electronics*, vol. 28, no. 5, pp. 2151-2169, 2013, doi: 10.1109/TPEL.2012.2212917.
- [2] B. Whitaker *et al.*, "A high-density, high-efficiency, isolated on-board vehicle battery charger utilizing silicon carbide power devices," *IEEE Transactions on Power Electronics*, vol. 29, no. 5, pp. 2606-2617, 2014, doi: 10.1109/TPEL.2013.2279950.
- [3] H. Sarnago, O. Lucía, R. Jiménez, and P. Gaona, "Differential-power-processing on-board-charger for 400/800-V battery architectures using 650-V super junction MOSFETs," in *Proc. of the IEEE Applied Power Electronics Conference and Exposition (APEC)*, 2021, pp. 564-568.
- [4] B. Li, Q. Li, F. C. Lee, Z. Liu, and Y. Yang, "A high-efficiency high-density wide-bandgap device-based bidirectional on-board charger," *IEEE Journal of Emerging and Selected Topics in Power Electronics*, vol. 6, no. 3, pp. 1627-1636, 2018, doi: 10.1109/JESTPE.2018.2845846.
- [5] P. Papamanolis, F. Krismer, and J. W. Kolar, "22 kW EV battery charger allowing full power delivery in 3-phase as well as 1-phase operation," in *Proc. of the International Conference on Power Electronics (ICPE - ECCE Asia)*, 2019, pp. 1-8, doi: 10.23919/ICPE2019-ECCEAsia42246.2019.8797063.
- [6] Y. Li, J. Schäfer, D. Bortis, J. W. Kolar, and G. Deboy, "Optimal synergetic control of a three-phase two-stage ultra-wide output voltage range EV battery charger employing a novel hybrid quantum series resonant DC/DC converter," in *Proc. of the IEEE Workshop on Control and Modeling for Power Electronics (COMPEL)*, 2020, pp. 1-11, doi: 10.1109/COMPEL49091.2020.9265732.

- [7] M. Antivachis, D. Bortis, L. Schrittwieser, and J. W. Kolar, "Three-phase buck-boost Y-inverter with wide DC input voltage range," in *Proc. of the IEEE Applied Power Electronics Conference and Exposition (APEC)*, 2018, pp. 1492-1499, doi: 10.1109/APEC.2018.8341214.
- [8] H. Sarnago, O. Lucía, S. Chhawchharia, D. Menzi, and J. W. Kolar, "Novel bidirectional universal 1-phase/3-phase-input unity power factor differential AC/DC converter," *IET Electronics Letters*, under review, 2023, doi: 10.22541/au.168318365.53360702/v1.
- [9] F. Krismer, and J. W. Kolar, "Efficiency-optimized high-current dual active bridge converter for automotive applications," *IEEE Transactions on Industrial Electronics*, vol. 59, no. 7, pp. 2745-2760, 2012, doi: 10.1109/TIE.2011.2112312.
- [10] F. Krismer, and J. W. Kolar, "Closed form solution for minimum conduction loss modulation of DAB converters," *IEEE Transactions on Power Electronics*, vol. 27, no. 1, pp. 174-188, 2012, doi: 10.1109/TPEL.2011.2157976.